

Experimental Validation of QoT Computation in Mixed 10G/100G Networks

*Original*

Experimental Validation of QoT Computation in Mixed 10G/100G Networks / Virgillito, Emanuele; Straullu, Stefano; Castoldi, Andrea; Bovio, Andrea; Rodriguez, Fransisco M.; Bratovich, Rudi; Pastorelli, Rosanna; Curri, Vittorio. - ELETTRONICO. - (2021), p. M5I.3. ( Asia Communications and Photonics Conference 2021 Shanghai China 24–27 October 2021) [10.1364/ACPC.2021.M5I.3].

*Availability:*

This version is available at: 11583/2976138 since: 2023-02-16T18:18:31Z

*Publisher:*

Optica Publishing Group

*Published*

DOI:10.1364/ACPC.2021.M5I.3

*Terms of use:*

This article is made available under terms and conditions as specified in the corresponding bibliographic description in the repository

*Publisher copyright*

Optica Publishing Group (formely OSA) postprint/Author's Accepted Manuscript

“© 2021 Optica Publishing Group. One print or electronic copy may be made for personal use only. Systematic reproduction and distribution, duplication of any material in this paper for a fee or for commercial purposes, or modifications of the content of this paper are prohibited.”

(Article begins on next page)



model [15] for coherent, DU transmission does not apply for the 10G-to-100G XPM estimation, as the interaction between XPM and random birefringence becomes significant due to the random 10G state of polarization evolution. Such scenario strongly impacts 100G QoT, commonly controlled setting a guardband between 10G comb and 100G channels [2, 12]. In [5, 6] we have proposed and validated a simple approach to model the 10G-to-100G XPM as a further additive noise source (Fig. 1a) by means of split-step Fourier method (SSFM) simulations, as the NLPN part is recovered by the CPE stage [4]. Hence, the overall 10G-to-100G SNR degradation contribution sums in parallel to the GSNR with other SNR degradations due to the ASE and NLI.

$$\text{SNR}_{\text{NL},10\text{G},k,n}^{-1} = \sin^2 2\theta_n E[|\sin \Delta\phi_{k,n}|^2] \quad (1)$$

Eq. 1 gives the 10G-to-100G XPM SNR degradation originating from the  $k$ -th 10G channel and the  $n$ -th span of the crossed OLS.  $\theta_n$  is a birefringence equivalent polarization rotation for the  $n$ -th span and  $\Delta\phi_{k,n}$  depends on the polarization aligned phase noise introduced by the  $k$ -th 10G channel on the  $n$ -th span [5, 6]. The model assumes that random birefringence couples the  $\Delta\phi_{k,n}$  phase noise term in an additive polarization crosstalk noise.  $\Delta\phi_{k,n}$  has been shown to converge after some spans to a worst-case asymptotic value depending only on the inline residual dispersion  $D_{\text{RES,IL}}$  left at the span end rather than on the dispersion coefficient [5, 6], so that the model is worst-case and *spatially disaggregated*, i.e. the QoT degradation introduced on the  $n$ -th span depends solely on the span itself and exhibits no coherency w.r.t. the propagation history. The model is also *spectrally disaggregated*, i.e. the QoT degradation on the 100G by the  $k$ -th 10G pump does not require knowledge of the other 10G pumps. Hence, the overall degradation after  $N_s$  spans due to  $N_p$  10G pumps is given by the inverse SNR sum of the Eq. 1 terms:

$$\text{SNR}_{\text{NL},10\text{G}}^{-1} = \sum_{k=1}^{N_p} \sum_{n=1}^{N_s} \text{SNR}_{\text{NL},10\text{G},k,n}^{-1} \quad (2)$$

The spectral and spatial disaggregation properties, as outlined in Fig. 1b, represent a strong requirement for network orchestration since they reduce the PCE complexity in real-time lightpath deployment operations.

### 3. Experimental Setup and Validation

We here report the methodology and results of the experimental validation of the model carried out synergistically with SM-Optics laboratories. The 16-span setup is outlined in Fig. 2a. 17 amplified nodes are cascaded, using G.652 fiber spans with average fiber lengths of 50 km. The dispersion map is set to the nominal value of  $D_{\text{RES,IL}} = 50$  ps/nm by placing a DCU at the end of each fiber span. The actual  $D_{\text{RES,IL}}$  values at the end of the  $n$ -th span may deviate significantly from the nominal value due to DCU granularity, however they were arranged in such a way that their average value is of 49.2 ps/nm. Terminal 2 is used to loopback the system, in order to use the same nodes twice (in different directions). Two power shaper nodes are used in the chain to control channel power equalization. Amplifier gain is set to transparency, so that the variation of the first node power is equally reflected in all subsequent spans, guaranteeing an equal power per channel of -1 dBm in all fiber spans. The OLS has been loaded with 12x 10G channels spaced 50 GHz apart, placed at a guardband of 100 GHz away from a commercial 100G probe with 28 GBaud PM-QPSK modulation. The DSP includes CPE algorithms which are able to substantially recover the NLPN. The first step has been to characterize the 100G performance when operating within the linear regime. This was performed by propagating the 100G probe alone with a sufficiently low channel power in order to avoid non-linearity generation. The signal is then progressively loaded at the receiver with ASE noise. We thus obtained the curve of the  $\text{OSNR}_{\text{lin}}$  set by noise loading and measured with an OSA, and its corresponding BER measured by error counting. In such conditions,  $\text{OSNR}_{\text{lin}}$  thus represents the overall available GSNR for that transceiver, as no NLI noise is present. Secondly, we characterize the single-channel non-linear

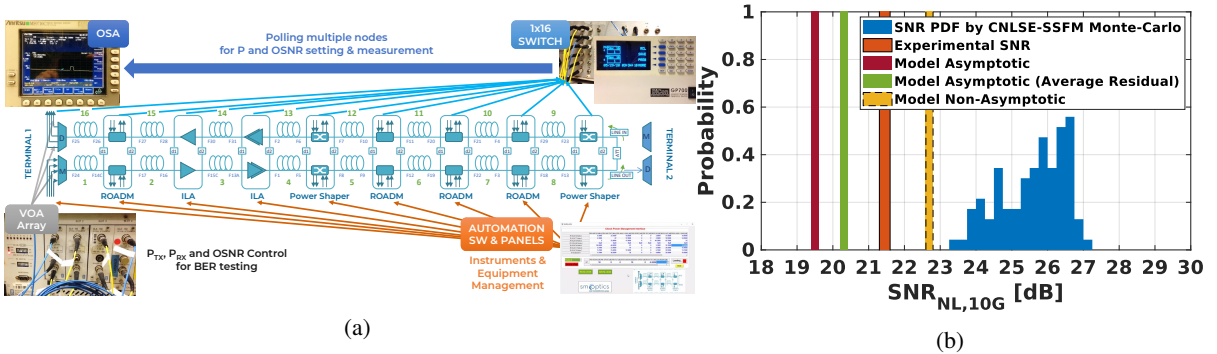


Fig. 2: (a) Description of the 16 span OLS experimental setup using commercial equipment. (b) 10G-to-100G XPM experimental SNR of Fig. 2a setup compared to PDF estimated by CNLSE-SSFM simulations and analytical model results.

interference (SCI) by setting the 100G probe power to the -1 dBm target level and repeated the noise loading process to obtain the  $\text{OSNR}_{\text{SCI}}$  (by OSA) vs BER curve. Since the OSA only catches up the ASE noise and we assume the SCI as additive noise, its QoT degradation  $\text{SNR}_{\text{SCI}}$  is obtained by the inverse SNR difference as  $(1/\text{OSNR}_{\text{lin}} - 1/\text{OSNR}_{\text{SCI}})^{-1}$ , after interpolation of the linearity and SCI curves to the same BER value. We then lit up the 12x 10G pumps comb and repeated the process to obtain the aggregated  $\text{SNR}_{\text{SCI,XPM}}$  due to SCI and 10G-to-100G XPM as  $(1/\text{OSNR}_{\text{lin}} - 1/\text{OSNR}_{\text{SCI,XPM}})^{-1}$ . Finally, the experimental  $\text{SNR}_{\text{NL,10G}}$  is obtained by removing the SCI contribution as the inverse difference in linear units  $(1/\text{SNR}_{\text{SCI,XPM}} - 1/\text{SNR}_{\text{SCI}})^{-1}$  and averaging over the noise loading points. Fig.2b reports the experimental  $\text{SNR}_{\text{NL,10G}}$  compared to the model results and its probability density function (PDF) estimation (in blue) obtained with an SSFM-based Monte-Carlo simulation campaign that averages over 100 realizations of the random birefringence polarization rotation process solving the coupled non-linear Schroedinger equation (CNLSE) [13]. This was performed upon the same experimental setup using our FFSS [7] simulation framework, where the 10G-to-100G XPM has been isolated with ideal noiseless amplifiers and a sufficiently low 100G probe power, in order to intercept the theoretical worst case of the phenomenon. Both the experimental and model values are conservative w.r.t. the SSFM minimum SNR, with a 2.1 dB experimental deviation, presumably due to the measurement uncertainties deriving from the differential measuring process and amplifier working points. The yellow bar reports the model estimation using the non-asymptotic  $\Delta\phi_{k,n}$  phase noise values obtained from polarization aligned simulations on identical residuals sequence to the experimental setup. As this adheres to the actual noise accumulation, there is a difference of only 0.67 dB from the SSFM theoretical worst case, confirming a good accuracy of the modeling approach, although being non-conservative w.r.t. the experimental value. The other two bars report the worst-case version of the model, obtained using the asymptotic  $\Delta\phi_{k,n}$  values. The red uses the asymptotic  $\Delta\phi_{k,n}$  corresponding to the exact  $D_{\text{RES,IL}}$  values found at the end of each experimental setup span. The green assumes that all the spans have  $D_{\text{RES,IL}}$  equal to the 49.2 ps/nm average residual value. Both bars deliver a conservative value w.r.t. the experimental one, with a gap of 1.83 and 1.00 dB, respectively, which we consider an acceptable accuracy when estimating a single part of the total non-linear effects in this transmission scenario. This confirms a good match of the QoT-E with a commercial equipment setup and still allows conservative operation, even when the exact residual dispersion distribution of the deployed OLS is not known and one should rely only on its nominal average value.

#### 4. Conclusions

We have experimentally validated a QoT-E for conservative estimation of the QoT degradation induced by the non-linear crosstalk from 10G channels to a 100G coherent channel in a *spectrally* and *spatially* disaggregated manner.

#### Acknowledgements

We acknowledge SM-Optics for carrying out the experimental activity and continuous support.

#### References

1. V. Curri, *Software-defined WDM optical transport in disaggregated open optical networks*, in *ICTON 2020*, (IEEE 2020), paper We.C2.1, doi: 10.1109/ICTON51198.2020.9203450
2. A. Carena *et al.*, *Guard-Band for 111 Gbit/s coherent PM-QPSK channels on legacy fiber links carrying 10 Gbit/s IMDD channels*, in *OFC 2009*, (OSA, 2009), paper OThR7, doi: 10.1364/OFC.2009.OThR7
3. E. Virgillito *et al.*, *Quality of Transmission Estimator Enabling the Transparency Paradigm in Legacy IMDD Networks*, in *ICTON 2018*, (IEEE, 2018), paper Mo.B3.2, doi: 10.1109/ICTON.2018.8473720
4. E. Virgillito *et al.*, *Propagation Effects in Mixed 10G-100G Dispersion Managed Optical Links*, in *ICTON 2019*, (IEEE 2019), paper We.D1.5, doi: 10.1109/ICTON.2019.8840162
5. E. Virgillito *et al.*, *Non-linear SNR degradation of mixed 10G/100G transmission over dispersion-managed networks*, in *ICTON 2020*, (IEEE 2020), paper We.C2.5, doi: 10.1109/ICTON51198.2020.9203204
6. E. Virgillito *et al.*, *QoT Computation for 100G Lightpaths Routed on 10G-loaded Dispersion-Managed Network Segments*, in *ICECC 2021*, (IEEE 2021), paper 121
7. D. Pileri *et al.*, *FFSS: The fast fiber simulator software*, in *ICTON 2017*, (IEEE, 2017), paper We.B1.5, doi: 10.1109/ICTON.2017.8025002
8. J. Kundrač *et al.*, *Opening up ROADMs: Let Us Build a Disaggregated Open Optical Line System*, *IEEE J. Lightwave Technol.* vol. 37, no. 16, 4041–4051 (2019), doi: 10.1109/JLT.2019.2906620
9. A. Ferrari *et al.*, *GNPy: an open source application for physical layer aware open optical networks*, *J. Opt. Commun. Netw.* vol. 12, no. 6, C31–C40 (2020), doi: 10.1364/JOCN.382906
10. M. Filer *et al.*, *Toward Transport Ecosystem Interoperability Enabled by Vendor-Diverse Coherent Optical Sources Over an Open Line System*, *J. Opt. Commun. Netw.* vol. 10, no. 2, A216–A224 (2018), doi: 10.1364/JOCN.10.00A216
11. M. Filer *et al.*, *Multi-Vendor Experimental Validation of an Open Source QoT Estimator for Optical Networks*, *IEEE J. Lightwave Technol.* vol. 36, no. 15, 3073–3082 (2018), doi: 10.1109/jlt.2018.2818406
12. O. Bertran-Pardo *et al.*, *Overlaying 10 Gb/s Legacy Optical Networks With 40 and 100 Gb/s Coherent Terminals*, *IEEE J. Lightwave Technol.* vol. 30, no. 14, 2367–2375 (2012), doi: 10.1109/JLT.2012.2198432
13. D. Marcuse *et al.*, *Application of the Manakov-PMD equation to studies of signal propagation in optical fibers with randomly varying birefringence*, *IEEE J. Lightwave Technol.* vol. 15, no. 9, 1735–1746 (1997), doi: 10.1109/50.622902
14. J. Santos *et al.*, *On the Impact of Deploying Optical Transport Networks Using Disaggregated Line Systems*, *J. Opt. Commun. Netw.* vol. 10, no. 1, A60–A68 (2018), doi: 10.1364/JOCN.10.000A60
15. P. Poggiolini, *The GN-model of fiber non-linear propagation and its applications*, *IEEE J. Lightwave Technol.* vol. 32, no. 4, 694–721 (2014), doi: 10.1109/JLT.2013.2295208